LETTER

Additive threats from pathogens, climate and land–use change for global amphibian diversity

Christian Hof[1,2], Miguel B. Araújo[1,2,3], Walter Jetz[4] & Carsten Rahbek[1]

Amphibian population declines far exceed those of other vertebrate groups, with 30% of all species listed as threatened by the International Union for Conservation of Nature[1–3]. The causes of these declines are a matter of continued research, but probably include climate change, land-use change and spread of the pathogenic fungal disease chytridiomycosis[1,4,5]. Here we assess the spatial distribution and interactions of these primary threats in relation to the global distribution of amphibian species. We show that the greatest proportions of species negatively affected by climate change are projected to be found in Africa, parts of northern South America and the Andes. Regions with the highest projected impact of land-use and climate change coincide, but there is little spatial overlap with regions highly threatened by the fungal disease. Overall, the areas harbouring the richest amphibian faunas are disproportionately more affected by one or multiple threat factors than areas with low richness. Amphibian declines are likely to accelerate in the twenty-first century, because multiple drivers of extinction could jeopardize their populations more than previous, mono-causal, assessments have suggested.

Amphibians are experiencing population declines in all regions of the world[2,6]. Causes for this global decline have been identified. Among the highest ranking threats are anthropogenic land-use changes, leading to habitat destruction and fragmentation, and the fatal disease chytridiomycosis, which is caused by the chytrid fungus *Batrachochytrium dendrobatidis*. Other threats include climate change, which may interact with chytridiomycosis, environmental pollution, direct exploitation for the food, medicine and pet trades, increase in ultraviolet-B irradiation due to anthropogenic ozone depletion, and the spread of invasive species[4,5].

Many studies have assessed how these threats affect amphibian populations and how they may interact at local and regional scales[7–10]. Recent assessments have used bioclimatic envelope models to project climate change impacts on amphibian diversity on a continental scale[11,12]. Attempts have also been made to assess the relative importance of different threats for large groups of species[13,14], but not in a spatially explicit way. Several hypotheses have suggested that there may be interactions of chytridiomycosis with land-use change[15] and climate change[9], yet no final consensus has been reached[10,16]. Preliminary models of the global geography of chytridiomycosis under climate change have been provided[17], but an integrative, analytical, spatially explicit assessment at a global scale of the spatial interactions of the most severe threats is urgently needed.

Using a nearly complete global data set of 5,527 amphibian species, we elucidate how the spatial interaction at the global scale of three important threats (climate change, chytridiomycosis and land-use change, see Methods) could affect global amphibian diversity between a baseline period (1980) and late in the present century (2080). Threat from future climate change was estimated as the proportion of species locally losing climatic suitability ('climate losers') per area, as given by species-specific bioclimatic models (see Methods). Because the spatial distribution of species richness varies considerably among the three amphibian orders Anura (frogs and toads, 'frogs' hereafter), Caudata (salamanders and newts, 'salamanders') and Gymnophiona ('caecilians') (Fig. 1a), we conducted climate change analyses separately for each group. Threat from chytridiomycosis was quantified as the future probability of occurrence of *B. dendrobatidis* from a bioclimatic model projection[17]. Lastly, estimates of future land-use change (that is, changes from natural to human-encroached land cover) were based on the projections of the Millennium Ecosystem Assessment[18–20].

The three major global threats to amphibians exhibit characteristic, yet disparate geographic patterns (Fig. 1b–d). For frogs, regions with a high projected impact of climate change (regions where high proportions of climate losers in 2080 coincide with a high level of species richness) are the northern Andes and parts of the Amazon and the Cerrado in South America, large areas of sub-Saharan tropical Africa, and a small region in South East Asia (Fig. 1b and Supplementary Fig. 1a). In the northern Andes, which harbour the greatest frog diversity worldwide, the proportion of probable climate losers reaches 166 species (73% of the local frog fauna). Globally, the proportion of frogs likely to become climate losers measured as average per grid cell is 54% (± 10% (standard deviation, s.d.)). For salamanders, western North America, northern Central America and southern and south-eastern Europe are the regions projected to be most heavily affected by climate change, as are some areas in northern South America for caecilians (Fig. 1b). In several areas of Central America, up to 21 species (66% of the local salamander fauna) are projected to lose climatic suitability (global mean ~56% ± 15% s.d.) (Fig. 1b). The regions with the highest projected probability of occurrence of chytridiomycosis are located in mostly temperate climates as well as mountainous and coastal regions (Fig. 1c). Areas with high projected land-use change are mainly found in tropical Central and South America, tropical Africa and montane parts of central and southern Asia (Fig. 1d).

Geographic coincidence in the intensity of the three types of threat is highly uneven and varies strongly among the three amphibian orders (Figs 1b–d and 2). Within the range occupied by frogs, the spatial overlap between the top 25% affected grid cells for the three threat types is small: 6.1% of these cells (out of a 25% possible) overlap for chytridiomycosis and climate change, 9.1% for climate change and land-use change and 8.6% for chytridiomycosis and land-use change (Figs 2 and 3; see Supplementary Table 1 for sensitivity analyses and spatial null model tests of overlap; see also Methods and Supplementary Methods for further details). The small degree of overlap between areas of highest impact from chytridiomycosis and climate change arises because of the strong association of *B. dendrobatidis* with humid and cool conditions found in temperate regions[21] and cool tropical high mountains, whereas the negative impacts from climate change are more prominent in the warm and wet tropics (see Fig. 1a). For salamanders, the comparable figures for spatial overlap are 12.2%, 4.6% and 10.0%, respectively (Fig. 3 and Supplementary Table 1). Globally, more than half of the distributional area of each of the three

[1]Center for Macroecology, Evolution and Climate, Department of Biology, University of Copenhagen, Universitetsparken 15, 2100 Copenhagen Ø, Denmark. [2]Department of Biodiversity and Evolutionary Biology, National Museum of Natural Sciences, CSIC, C/José Gutiérrez Abascal 2, 28006 Madrid, Spain. [3]Rui Nabeiro Biodiversity Chair, CIBIO, University of Évora, Largo dos Colegiais, 7000 Évora, Portugal. [4]Department of Ecology and Evolutionary Biology, Yale University, 165 Prospect Street, New Haven, Connecticut 06520-8106, USA.
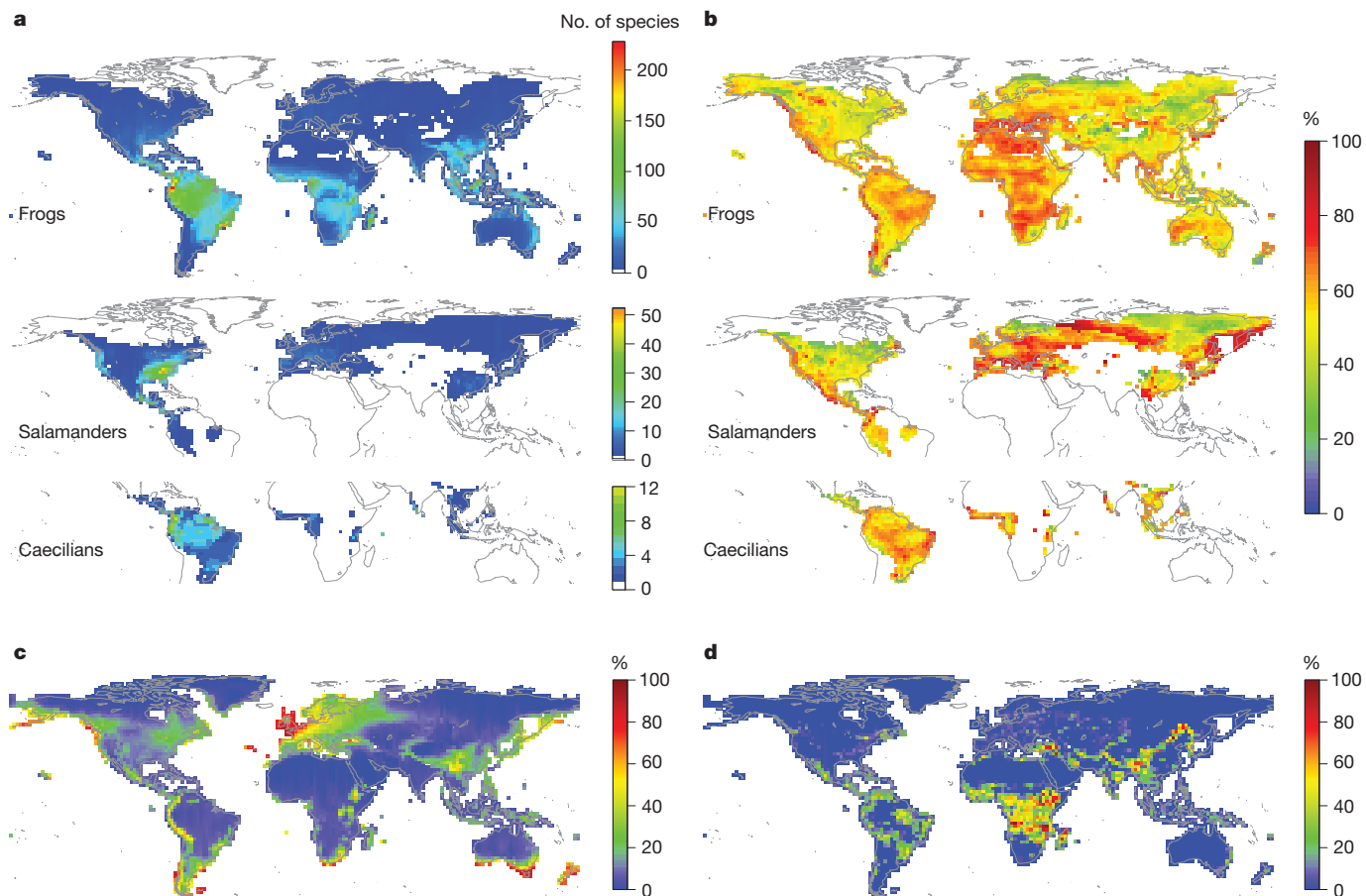
Figure 1 | Current amphibian species richness and the intensity of three factors threatening global amphibian diversity projected for the year 2080. **a**, Spatial variation of species richness (number of species per grid cell) of frogs ($n = 4,875$), salamanders ($n = 508$) and caecilians ($n = 144$). **b**, Intensity of threat from climate change, given as the proportion of species projected to lose climatic suitability in a given area (arithmetic mean across 14 GCMs, 3 emission scenarios and 3 modelling algorithms). **c**, Intensity of threat from chytridiomycosis, given as the projected probability of occurrence of *B. dendrobatidis* (arithmetic mean across 3 GCMs and 2 emission scenarios, data from ref. 17). **d**, Intensity of threat from land-use change, given as the proportion of a given area projected to be converted from a natural to an anthropogenic state (arithmetic mean across 4 scenarios, data from ref. 19). For further details on the quantification of threat intensities, see Methods. White areas in panels **a** and **b** indicate the absence of a given amphibian order.

amphibian orders is likely to be highly affected by at least one of the three major threat factors. When only regions with the highest species richness are considered, then about two thirds of the areas with the richest frog and salamander faunas (half of the area for caecilians) are projected to become heavily affected by 2080 (Fig. 4).
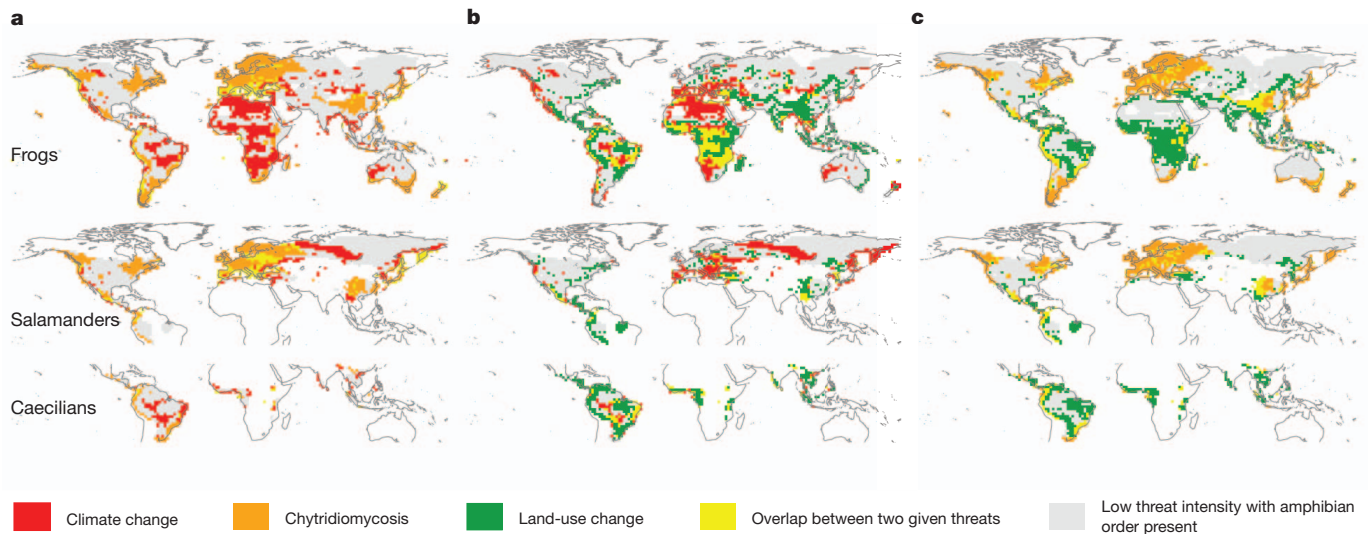
Several critical assumptions are inevitable when conducting global assessments like ours. Although a careful investigation of some of the methodological uncertainties in our study broadly confirms the consistency of our findings (see Methods, Supplementary Methods and Supplementary Discussion), several limitations are important.

First, much uncertainty exists in ensemble forecasting as illustrated by the results produced by our use of 14 different global climate models (GCMs) and three bioclimatic envelope modelling algorithms (Supplementary Figs 8–12). Although we explicitly examined this variation, results are contingent on the methods used and future modelling might provide further insights. Second, other threats not investigated here may also cause declines in amphibian populations, including pollution, direct exploitation, spread of invasive species, or increased ultraviolet-B irradiation[5]. These additional factors give reason for further concern, especially when they interact with one another[4]. Third,
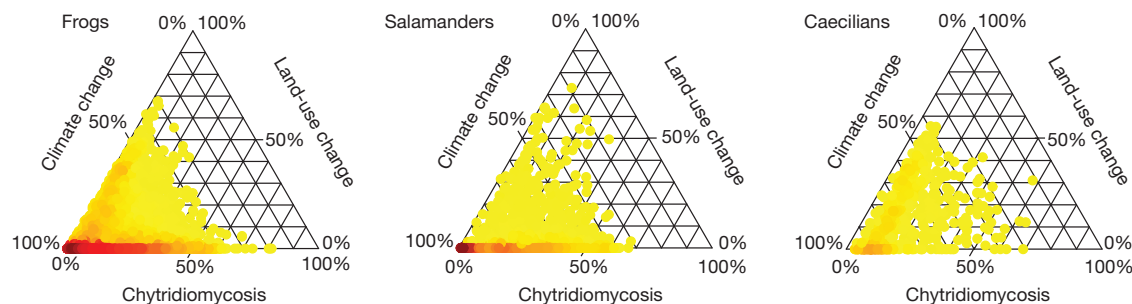
Figure 2 | Relationships among the intensities of the three main factors threatening global amphibian diversity. Each point refers to one grid cell in Fig. 1 and represents the relative intensity of each of the three threats when considered jointly: climate change (proportion of species losing climatic suitability); chytridiomycosis (probability of occurrence of chytridiomycosis); and land-use change. For details on the quantification of threat intensities, see Fig. 1 and Methods. Values of threat intensity are standardized to vary between 0 and 100%, and then transformed into relative proportions to add up to 100% (division by the sum of the three threat intensities). Darker colours indicate higher point densities.

🟥 Climate change	🟧 Chytridiomycosis	🟩 Land-use change
🟨 Overlap between two given threats		⬜ Low threat intensity with amphibian order present

Figure 3 | Spatial distribution and pairwise overlap of the three main factors threatening global amphibian biodiversity, projected for the year 2080. **a**, Climate change and chytridiomycosis. **b**, Climate change and land-use change. **c**, Chytridiomycosis and land-use change. Colours indicate areas of particularly high threat intensity. These areas are defined as the 25% of all grid cells with (1) the highest proportion of species projected to lose climatic suitability, (2) the highest projected probability of occurrence of chytridiomycosis and (3) the highest proportion of land projected to be converted from a natural to an anthropogenic state. For other details see Fig. 1.

modelled presence of chytridiomycosis does not always cause local declines or extinctions and interspecific as well as regional differences in amphibian susceptibility to chytridiomycosis exist[22]. Fourth, the spatial resolution of our analysis is relatively coarse, yet several factors allow

High species richness	
🟦 0 threats	⬜ Low species richness
🟨 1 threat	
🟧 2 threats	
🟥 3 threats	
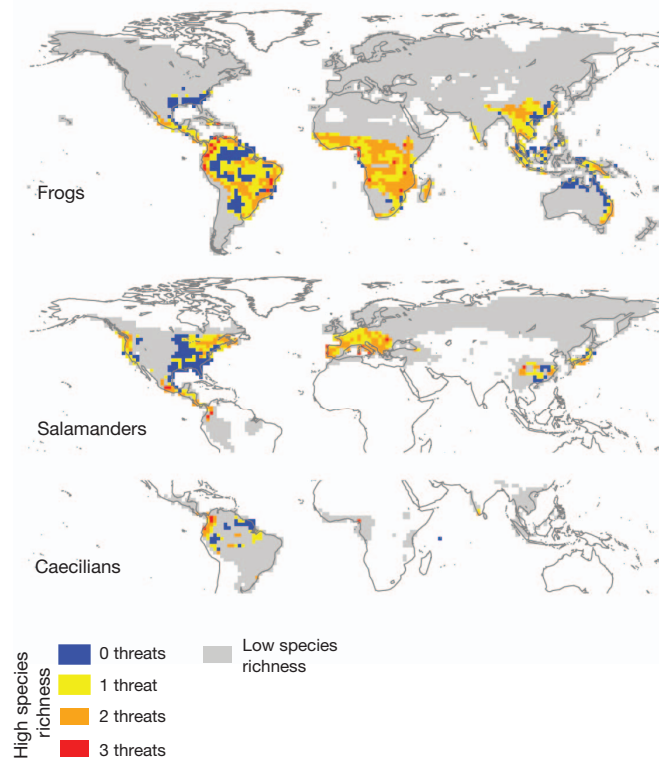
Figure 4 | Spatial overlap between areas with the highest amphibian species richness and the main factors threatening global amphibian diversity, projected for 2080. Areas with the highest species richness are defined as the 25% of all grid cells with the highest number of species. Areas where high levels of species richness coincide with high intensity of 1–3 of the main factors threatening amphibian diversity are coloured in yellow, orange and red, respectively (blue: no coincidence of high richness and high threat intensity). For definition of 25% areas of high threat intensity and further details see Figs 1 and 3.

population persistence at finer scales (see also discussion in refs 23, 24). In particular, our analyses disregard dispersal, biotic interactions and adaptive potential, and rely on the assumption that coarse-scale projections from bioclimatic envelope models provide a good surrogate for species' climatic requirements at finer scales. However, in some cases, species might persist owing to increased climatic stability in fine-grain refugia[25], or to local adaptations of amphibian populations[26]. Our projections thus provide measurements of the exposure of global amphibian species distributions to key threatening processes but, because the species' responses to these threats are not investigated, projections overestimate the impacts of multiple threats on the persistence of local amphibian populations (see also Supplementary Discussion).

Despite these uncertainties, our results reveal an intriguing pattern of non-overlap between key threatening factors. The implication is that risk assessments focusing on a single threat, such as just climate change or only chytridiomycosis, are probably picturing an optimistic view. As such, they fail to identify the key actions required to curb the ongoing global decline in amphibian diversity. The low coincidence between regions projected to have high prevalence of chytridiomycosis and climate or land-use change emphasizes the potential for silent extinctions away from the regions where the current human footprint is larger. In turn, the higher coincidence between land-use and climate change highlights the existence of potential synergies between the two threatening factors that are often neglected[18,27,28]. The substantial overlap of threats with many of the world's centres of amphibian richness further underlines the pessimistic long-term perspective for global amphibian diversity[1,5]. It reinforces the realization that prioritization of conservation efforts needs to be based on knowledge of the spatial distribution both of the different key threats and of biodiversity.

METHODS SUMMARY

To identify the regions with the highest projected impacts of climate change on amphibian species, we fitted three familiar bioclimatic models for each of 5,527 species using an ensemble forecasting framework[29]. Climate data were extracted from 14 different GCMs (Supplementary Table 2)[30] under three emission scenarios. Across 5,041 2×2 degrees latitude–longitude cells, we identified species projected to lose climatic suitability in each grid cell ('climate losers') in 2080 compared with baseline conditions (1980). We then mapped the proportion of climate losers out of the total number of species per grid cell across the world. The probability of occurrence of *B. dendrobatidis* was obtained from a climate-based ensemble modelling projection (data from ref. 17). To estimate land-use change, we used the proportion of a grid cell projected to be actively transformed by humans in the presence of (but

not necessarily driven by) a changing climate (data from ref. 19; procedure following ref. 27).

Regions with highest projected impacts of climate change were identified as the 25% of the grid cells with the highest proportion of losers for each amphibian order. We also used the 25% threshold to identify the areas with the highest species richness, as well as the regions with the highest projected incidence of chytridiomycosis and the highest projected land-use change in 2080. We repeated the analyses using threshold levels of 20% and 10% to assess the consistency of our results. Spatial overlap among grid cells projected to be most affected was assessed by pairwise comparisons of the three threat factors, and also in relation to the distribution of regions with the highest levels of species richness.

Full Methods and any associated references are available in the online version of the paper at www.nature.com/nature.

1. Stuart, S. N. et al. Status and trends of amphibian declines and extinctions worldwide. *Science* **306,** 1783–1786 (2004).
2. IUCN. *An Analysis of Amphibians on the 2008 IUCN Red List* ⟨http://www.iucnredlist.org/initiatives/amphibians⟩ (2008).
3. Wake, D. B. & Vredenburg, V. T. Are we in the midst of the sixth mass extinction? A view from the world of amphibians. *Proc. Natl Acad. Sci. USA* **105,** 11466–11473 (2008).
4. Blaustein, A. R. & Kiesecker, J. M. Complexity in conservation: lessons from the global decline of amphibian populations. *Ecol. Lett.* **5,** 597–608 (2002).
5. Beebee, T. J. C. & Griffiths, R. A. The amphibian decline crisis: a watershed for conservation biology? *Biol. Conserv.* **125,** 271–285 (2005).
6. Houlahan, J. E., Findlay, C. S., Schmidt, B. R., Meyer, A. H. & Kuzmin, S. L. Quantitative evidence for global amphibian population declines. *Nature* **404,** 752–755 (2000).
7. Becker, C. G., Fonseca, C. R., Haddad, C. F. B., Batista, R. F. & Prado, P. I. Habitat split and the global decline of amphibians. *Science* **318,** 1775–1777 (2007).
8. Bosch, J., Carrascal, L. M., Duran, L., Walker, S. & Fisher, M. C. Climate change and outbreaks of amphibian chytridiomycosis in a montane area of Central Spain; is there a link? *Proc. R. Soc. Lond. B* **274,** 253–260 (2007).
9. Pounds, J. A. et al. Widespread amphibian extinctions from epidemic disease driven by global warming. *Nature* **439,** 161–167 (2006).
10. Lips, K. R., Diffendorfer, J., Mendelson, J. R. & Sears, M. W. Riding the wave: reconciling the roles of disease and climate change in amphibian declines. *PLoS Biol.* **6,** e72 (2008).
11. Lawler, J. J., Shafer, S. L. & Blaustein, A. R. Projected climate impacts for the amphibians of the Western Hemisphere. *Conserv. Biol.* **24,** 38–50 (2010).
12. Araújo, M. B., Thuiller, W. & Pearson, R. G. Climate warming and the decline of amphibians and reptiles in Europe. *J. Biogeogr.* **33,** 1712–1728 (2006).
13. Bielby, J., Cooper, N., Cunningham, A. A., Garner, T. W. J. & Purvis, A. Predicting susceptibility to future declines in the world's frogs. *Conservation Letters* **1,** 82–90 (2008).
14. Sodhi, N. S. et al. Measuring the meltdown: drivers of global amphibian extinction and decline. *PLoS One* **3,** e1636 (2008).
15. Becker, C. G. & Zamudio, K. R. Tropical amphibian populations experience higher disease risk in natural habitats. *Proc. Natl Acad. Sci. USA* **108,** 9893–9898 (2011).
16. Rohr, J. R., Raffel, T. R., Romansic, J. M., McCallum, H. & Hudson, P. J. Evaluating the links between climate, disease spread, and amphibian declines. *Proc. Natl Acad. Sci. USA* **105,** 17436–17441 (2008).
17. Rödder, D., Kielgast, J. & Lötters, S. Future potential distribution of the emerging amphibian chytrid fungus under anthropogenic climate change. *Dis. Aquat. Organ.* **92,** 201–207 (2010).
18. van Vuuren, D. P., Sala, O. E. & Pereira, H. M. The future of vascular plant diversity under four global scenarios. *Ecol. Soc.* **11,** 25 (2006).
19. Alcamo, J. et al. *Global Change Scenarios of the 21st Century, Results from the IMAGE 2.1 Model* 3–96 (Elsevier, 1998).
20. Millennium Ecosystem Assessment. *Ecosystems and Human Well-Being: Scenarios.* (Island, 2005).
21. Daszak, P., Cunningham, A. A. & Hyatt, A. D. Infectious disease and amphibian population declines. *Divers. Distrib.* **9,** 141–150 (2003).
22. Kilpatrick, A. M., Briggs, C. J. & Daszak, P. The ecology and impact of chytridiomycosis: an emerging disease of amphibians. *Trends Ecol. Evol.* **25,** 109–118 (2010).
23. Hof, C., Rahbek, C. & Araújo, M. B. Phylogenetic signals in the climatic niches of the world's amphibians. *Ecography* **33,** 242–250 (2010).
24. Hof, C., Levinsky, I., Araújo, M. B. & Rahbek, R. Rethinking species' ability to cope with rapid climate change. *Glob. Change Biol.* **17,** 2987–2990 (2011).
25. Ashcroft, M. B. Identifying refugia from climate change. *J. Biogeogr.* **37,** 1407–1413 (2010).
26. Phillimore, A. B., Hadfield, J. D., Jones, O. R. & Smithers, R. J. Differences in spawning date between populations of common frog reveal local adaptation. *Proc. Natl Acad. Sci. USA* **107,** 8292–8297 (2010).
27. Jetz, W., Wilcove, D. S. & Dobson, A. P. Projected impacts of climate and land-use change on the global diversity of birds. *PLoS Biol.* **5,** e157 (2007).
28. Beaumont, L. J. et al. Impacts of climate change on the world's most exceptional ecoregions. *Proc. Natl Acad. Sci. USA* **108,** 2306–2311 (2011).
29. Araújo, M. B. & New, M. Ensemble forecasting of species distributions. *Trends Ecol. Evol.* **22,** 42–47 (2007).
30. Meehl, G. A. et al. The WCRP CMIP3 multimodel dataset: a new era in climate change research. *Bull. Am. Meteorol. Soc.* **88,** 1383–1394 (2007).

METHODS

Data. We fitted bioclimate envelope models (BEMs) for 5,527 amphibian species from the three amphibian orders Anura (frogs and toads), Caudata (salamanders and newts) and Gymnophiona (caecilians), which for simplicity are henceforth referred to as frogs, salamanders and caecilians. Distribution data were compiled from the Global Amphibian Assessment[31]. Polygons of species' ranges were resampled to a 2 × 2 degree latitude–longitude grid (referred to as the 2°-grid) including 5,041 terrestrial cells (for maps of species richness, see Fig. 1a). This resolution approximates the average of the original resolutions of the climate data sets (see later).

Climatic data were obtained from the World Climate Research Programme (WCRP) Coupled Model Intercomparison Project phase 3 (CMIP3) multi-model data set[30] of the Fourth Intergovernmental Panel on Climate Change (IPCC) report. Data were derived from 14 coupled Atmosphere-Ocean GCMs and 3 emission scenarios (see Supplementary Table 2 for an overview of the used data sets). Using this series of GCMs we encompass a wide range of equilibrium climate sensitivity (ECS; 2.1–4.3 °C; see Supplementary Table 2 for details) and an array of original spatial resolutions, from 1.1 × 1.1 to 3.75 × 3.75 degrees latitude–longitude in the original sets. Outputs for each model were obtained for three SRES[32] emission scenarios A1B, A2 and B1, but A2 and B1 scenarios were not available for all of the GCMs (Supplementary Table 2; see ref. 33 for a description of the different scenario storylines). Inclusion of these three scenarios ensures that the models cover a wide range of likely climatic changes.

For each of the GCMs and emission scenarios, five climatic variables were obtained to characterize the baseline period (averaged across a 30-year time period from 1970 to 1999) that was used to calibrate the models. The same variables were then used to make projections into a 30-year time period between 2070 and 2099, subsequently referred to as 2080. The variables used were mean annual rainfall and precipitation seasonality, annual temperature range, minimum temperature and maximum temperature. These variables are known to impose constraints on amphibian physiology and survival[34] and are often used to model amphibian species distributions and richness[12,35]. All climate variables were resampled to the 2°-grid.

By using a global extent approach and given the grain of our analysis, we (1) avoid asserting artificial data quality by inappropriate downscaling of the climatic data, and (2) minimize the problem of false absences in the species distribution data[36] as many species in the data set have only been identified in a few localities, with no knowledge about the true occurrence of the species[2]. However, the coarse resolution precludes detailed local assessments of threat interactions and processes; therefore our focus is on documenting coarse spatial patterns.

Projections of the probability of occurrence of *B. dendrobatidis* were obtained from climate-based consensus projections previously described[17]. These projections (standardized probability of occurrence given by a consensus of MaxEnt BEMs across three GCMs and two emission scenarios; Supplementary Fig. 3) were resampled to the 2°-grid by weighted averaging. In contrast to the climate change and land-use change projections, for chytridiomycosis we did not use values of the change of the probability of occurrence, as many regions are not infected yet by chytridiomycosis, which makes the absolute value of probability of occurrence a better estimate of future risk of *B. dendrobatidis* infection. For the subsequent analyses, we used a consensus map calculated as the arithmetic mean across all the projections (Fig. 1b). Generally, averaging across different scenarios may be problematic. However, for practical reasons and because separate maps of the variation of the probability of chytridiomycosis occurrence for each combination of used GCM × scenario did not show strong differences in the spatial pattern (Supplementary Fig. 3), we used the consensus map.

For the projections of potential land-use change, we used data from the Millennium Ecosystem Assessment[20,37]. The Millennium Ecosystem Assessment uses four scenarios representing a variety of socio-economic and political futures to estimate future changes in the Earth's land-cover[27] ('Adapting Mosaic', 'Global Orchestration', 'Order from Strength' and 'TechnoGarden'[20]). The Millennium Ecosystem Assessment maps provide information on current and future distributions of 18 different land-cover types at a 0.5° latitude–longitude resolution. For a quantification of potential land-use change we identified grid cells that are projected to change from a natural to an anthropogenic land-cover state (change of any land-cover type to land-cover type 3 'cropland/permanent pasture') and calculated the proportion of area changed for each cell of our 2°-grid for 2080, as a consensus map (arithmetic mean across all four scenarios, Fig. 1c) and separately for each of the four scenarios (Supplementary Fig. 4). As for the projections of chytridiomycosis, for practical reasons and because a separate use of different Millennium Ecosystem Assessment scenarios does virtually not affect the results, we used the consensus map in the subsequent analyses.

Modelling. Three different modelling algorithms, Euclidean distance (ED), Mahalanobis distance (MD) and MaxEnt (MX), were used to run BEMs. These presence-only algorithms were selected owing to the large number of species with uncertain distributions or very small range sizes to be modelled (see also Supplementary Discussion). The two distance-based methods (ED and MD) measure the similarity of each species' occurrence to the mean (or centre) of the available climatic space. Accordingly species' niches are defined as circular (for ED) or elliptical (for MD) shapes in climatic hyperspace[38]. BioEnsembles, a computer software which is able to optimize and take advantage of high-speed parallel processing, was used to run the ED and MD models[39]. MaxEnt version 3.2.4[40,41], a machine-learning technique based on the principle of maximum entropy, was used to run the MX models. In MaxEnt, we used a regularization multiplier of 0.5 (a model parameter which allows for adjustment of the degree of model overfitting), because this value represents a balance between being able to fit models for species with very few records while avoiding an unreliable degree of overfitting.

For each of the 5,527 species, we ran each possible modelling combination (3 modelling algorithms × 14 GCMs × 3 scenarios × 2 time periods), which resulted in 1,260,156 models (note that for some GCMs only two scenarios were available, Supplementary Table 2). Standard BEM validation procedures were not applicable in our study (but note that a validation for future scenarios is in any case not possible[42]). However, we cautiously assessed patterns of variation in model results that may have resulted from different sources of uncertainty, such as species with small numbers of occurrence records, different modelling algorithms, and variation among GCMs that may result from different resolutions and equilibrium climatic sensitivities, as well as different emission scenarios (see Supplementary Discussion, also for discussion on model-inherent assumptions). All analyses were performed separately for frogs, salamanders and caecilians.

Processing of modelling results. We used a no-dispersal scenario as the basic underlying assumption for the further processing of the modelling results for two reasons. First, it is unlikely that amphibians will be able to fully track changes in climatic conditions by shifts of their distributional ranges[43], in particular when thinking of the coarse spatial scale of our analyses (see also our discussion of coarse data implications in the Supplementary Discussion). Second, and more importantly, the ranges of many species are extremely small (see Supplementary Fig. 2 for range-size frequency distributions). Because BEM projections can become unreliable for species with few occurrence records[44–46], we refrained from projecting a species' range into areas where the species does not currently occur. Furthermore, to avoid uncertainties associated with the choice of thresholds to convert raw model outputs (that is, distance to the optimal centroids or probabilities of occurrence) into binary estimates of presence and absence[47], we decided not to use any type of thresholding. Instead, following ref. 48, we used the change in climatic suitability that overlapped with species' current ranges and disregarded suitability or probability scores that did not overlap with existing records for the species. The change in climatic suitability was then calculated as the difference of the climatic suitabilities between current and future conditions (standardized MX probability of occurrence or 1 minus the raw distance (standardized between 0 and 1) for ED and MD, respectively; see Supplementary Fig. 5 for an example). This procedure was repeated for each model combination (algorithm × GCMs × scenarios) for each species. Despite the standardization of values of suitability change to a range from 0 to 1, the values are not quantitatively comparable across the different modelling algorithms, which is due to general differences in distance-based (ED, MD) and machine-learning (MX) algorithms as well as to software-inherent differences (for histograms and maps of the mean changes of suitability per grid cell, calculated as the means across all species, see Supplementary Figs 6 and 7). Therefore we used a qualitative approach to identify the regions with the strongest projected impacts of climate change on amphibian diversity[48]: for each model combination, we counted the number of species per grid cell that (1) lose climatic suitability ('climate losers': negative change in climatic suitability between current and future conditions), (2) gain climatic suitability ('climate winners': positive change in climatic suitability between current and future conditions) and (3) show no change in climatic suitability between current and future conditions. Note that doing so implies that species will be counted as 'climate loser' or 'climate winner' regardless of the magnitude of those changes, and that species may be identified as losers in one grid cell and as winners in another. However, as we only analyse these counts in categorical and aggregate form (that is, cells with the highest proportion of losers) we expect results to be robust to this simplification and further provide sensitivity analyses (see also Supplementary Discussion).

To identify the regions with the strongest projected impacts of climate change on amphibian diversity, we built consensus maps of the proportion of climate losers and then identified the 25% of all grid cells with the highest proportion of losers (Fig. 3a). Consensus maps were derived by calculating arithmetic means of the proportion of climate losers across all model combinations (algorithm × GCM × scenario) for 2080 (Fig. 1a).

Many studies have shown that species distribution modelling results can vastly differ when using different GCMs, emission scenarios and algorithms[49,50]. To

assess the uncertainties around the consensus, we mapped the proportion of losers separately as arithmetic means (1) across all combinations of GCM × algorithm per scenario (Supplementary Fig. 8), (2) across all combinations of GCM × scenario per algorithm (Supplementary Fig. 9A–C), (3) across all combinations of GCM × scenario per combination of two algorithms (Supplementary Fig. 9D–F), and (4) across all combinations of algorithm × scenario per GCM (Supplementary Fig. 10). Furthermore, following a novel uncertainty assessment protocol[51], we assessed the proportion of variation explained by different sources of uncertainty (algorithm, GCM, scenario, their interactions, and the residual uncertainty) by variance partitioning (SS proportion in 3-way ANOVAs; Supplementary Fig. 11), and mapped these proportions of uncertainty (see Supplementary Fig. 12, ref. 51 and Supplementary Discussion for details). In addition, we identified the 25% grid cells with the highest proportion of climate losers separately for each model combination and calculated the number of models per grid cell that identified this grid cell as one of the 25% with the highest proportion of losers. These overlap maps were constructed for each possible algorithm combination (ED × MD × MX; ED × MD, ED × MX, MD × MX; ED, MD, MX) to assess also the amount of uncertainty that is associated with the use of one, two or three modelling algorithms (Supplementary Fig. 13).

Spatial overlap of different threats. To investigate the spatial overlap of different threats for amphibian diversity, we identified the regions with the highest projected impact for each of the respective threat: 25% of all grid cells with the highest proportion of climate losers (red areas in Supplementary Fig. 1A), 25% of all grid cells with the highest probability of occurrence of *B. dendrobatidis* (orange areas in Supplementary Fig. 1B), and the grid cells with a projected land-use change of at least 25% of the total area (green areas in Supplementary Fig. 1C). All of these calculations were based on the consensus maps derived using the procedures explained above. For statistical analyses of threat overlap, see Supplementary Methods and Supplementary Table 1.

31. IUCN. *Global Amphibian Assessment* ⟨http://www.iucnredlist.org/initiatives/amphibians/⟩ (2004).
32. IPCC. *Special Report on Emissions Scenarios, Prepared for the Third Assessment Report* (IPCC, 2000).
33. IPCC. *Contribution of Working Group I to the Fourth Assessment Report of the Intergovernmental Panel on Climate Change: Summary for Policymakers* (IPCC, 2007).
34. Carey, C. & Alexander, M. A. Climate change and amphibian declines: is there a link? *Divers. Distrib.* **9,** 111–121 (2003).
35. Araújo, M. B. *et al.* Quaternary climate changes explain diversity among reptiles and amphibians. *Ecography* **31,** 8–15 (2008).
36. Hurlbert, A. H. & Jetz, W. Species richness, hotspots, and the scale dependence of range maps in ecology and conservation. *Proc. Natl Acad. Sci. USA* **104,** 13384–13389 (2007).
37. Millennium Ecosystem Assessment. *Ecosystems and Human Well-Being: Synthesis* (Island, 2005).
38. Farber, O. & Kadmon, R. Assessment of alternative approaches for bioclimatic modeling with special emphasis on the Mahalanobis distance. *Ecol. Modell.* **160,** 115–130 (2003).
39. Bioensembles: software for computer intensive ensemble forecasting of species distributions under climate change v. 1.0 (privately distributed, Madrid, Goiás, Évora, 2009).
40. Phillips, S. J., Anderson, R. P. & Schapire, R. E. Maximum entropy modeling of species geographic distributions. *Ecol. Modell.* **190,** 231–259 (2006).
41. Phillips, S. J. & Dudik, M. Modeling of species distributions with Maxent: new extensions and a comprehensive evaluation. *Ecography* **31,** 161–175 (2008).
42. Araújo, M. B., Pearson, R. G., Thuiller, W. & Erhard, M. Validation of species–climate impact models under climate change. *Glob. Change Biol.* **11,** 1504–1513 (2005).
43. Smith, M. A. & Green, D. M. Dispersal and the metapopulation paradigm in amphibian ecology and conservation: are all amphibian populations metapopulations? *Ecography* **28,** 110–128 (2005).
44. Stockwell, D. R. B. & Peterson, A. T. Effects of sample size on accuracy of species distribution models. *Ecol. Modell.* **148,** 1–13 (2002).
45. McPherson, J. M., Jetz, W. & Rogers, D. J. The effects of species' range sizes on the accuracy of distribution models: ecological phenomenon or statistical artefact? *J. Appl. Ecol.* **41,** 811–823 (2004).
46. Wisz, M. S. *et al.* Effects of sample size on the performance of species distribution models. *Divers. Distrib.* **14,** 763–773 (2008).
47. Nenzén, H. K. & Araújo, M. B. Choice of threshold alters projections of species range shifts under climate change. *Ecol. Modell.* **222,** 3346–3354 (2011).
48. Araújo, M. B., Alagador, D., Cabeza, M., Nogues-Bravo, D. & Thuiller, W. Climate change threatens European conservation areas. *Ecol. Lett.* **14,** 484–492 (2011).
49. Araújo, M. B., Whittaker, R. J., Ladle, R. J. & Erhard, M. Reducing uncertainty in projections of extinction risk from climate change. *Glob. Ecol. Biogeogr.* **14,** 529–538 (2005).
50. Pearson, R. G. *et al.* Model-based uncertainty in species range prediction. *J. Biogeogr.* **33,** 1704–1711 (2006).
51. Diniz-Filho, J. A. F. *et al.* Partitioning and mapping uncertainties in ensembles of forecasts of species turnover under climate change. *Ecography* **32,** 897–906 (2009).